

Supporting Information

Collaborative assembly of doxorubicin and galactosyl diblock glycopolymers for targeted drug delivery of hepatocellular carcinoma

Jianghua Li,^{a‡} Yang Zhang,^{a‡} Chao Cai,^{ab‡} Xiaozhi Rong,^{ab} Meng Shao,^a Jiarui Li,^a Chendong Yang^a and Guangli Yu^{ab*}*

^a Key Laboratory of Marine Drugs, Ministry of Education & Shandong Provincial Key Laboratory of Glycoscience and Glycotechnology, School of Medicine and Pharmacy, Ocean University of China, Qingdao 266003, China. E-mail addresses: caic@ouc.edu.cn (C. Cai), glyu@ouc.edu.cn

(G. Yu)

^b Laboratory for Marine Drugs and Bioproducts, Pilot National Laboratory for Marine Science and Technology (Qingdao), Qingdao 266237, China.

‡ These authors contributed equally.

Table of Contents

1. Measurements	S2
2. Synthesis and characterization of galactosyl monomer	S3
2.1 Synthesis of galactosyl monomer	S3
2.2 ¹ H NMR spectrum of related Compounds	S4
3. Temperature sensitivity of GN Vehicle III.	S6
4. Quantitative analysis of doxorubicin	S7
4.1 The method of quantitative analysis of doxorubicin.....	S7
4.2 Data about the quantitative analysis of doxorubicin	S9
5. In vitro biocompatibility evaluation	S12
6. In vivo activity evaluation	S13
7. Reference	S14

1. Measurements

¹H NMR spectra were recorded on an Agilent DD2 spectrometer (500 MHz). The chemical shifts of all the NMR spectra were reported in delta (δ) units and expressed as parts per million (ppm). The NMR spectra were referenced using TMS (0 ppm), residual CHCl₃ (¹H NMR δ = 7.26 ppm) and D₂O (¹H NMR δ = 4.79 ppm). For Fourier transform infrared spectroscopy (FT-IR) spectra collection, the dried sample was mixed with dried KBr and pressed to make transparent film for FT-IR measurements using a Nicolet Nexus 470 instrument (Thermo Electron Corp., Madison, WI, USA) with a frequency resolution of 1 cm⁻¹ and 64 scans between 4000 and 400 cm⁻¹. Zeta potential analysis of GN Vehicles I-IV were performed by dynamic light scattering measurement using the zetasizer Nanoparticle Analyser (Nano ZS 90; Malvern Instruments, Ltd., Malvern, United Kingdom). Transmission electron microscope (TEM) images of samples were obtained by a JEOL JSM 5410 transmission electron microscope (Japan) and statistics by Nano Measurer. Absorbance and fluorescence intensity measurements were performed by microplate reader Tecan *SparkControl*[™] V2.3.5. Confocal laser scanning microscope (CLSM) images were taken by a LSM 700 confocal scanning microscope (A1+A1R+, Nikon, Japan). Phenotype of zebrafish were taken by inverted fluorescence microscope (DM6000, Germany Leica).

2. Synthesis and characterization of galactosyl monomer

2.1 Synthesis of galactosyl monomer

Synthesis of β -D-galactopyranosylamine 2.² The reported procedure was applied to synthesize β -D-galactopyranosylamine. D (+)-galactose (1.8 g, ammonium carbamate (3.12 g, 4 eq) were dissolved in 40 mL CH₃OH and stirred at 37 °C for 48 h, then the precipitate was collected by filtration and washed with methanol (10 mL \times 3). The dried product was directly subjected to the next reaction without purification.

Synthesis of *N*-(prop-2-enoyl)- β -D-galactopyranosylamine 3.³ The dried β -D-galactopyranosylamine **2** obtained above and Na₂CO₃ (6 g, 5.5 eq) were dissolved in 120 mL of CH₃OH - H₂O (V: V, 1:1), the mixture was stirred at -5 °C in the low temperature freezing magnetic stirrer for 30 min, and then a solution of acryloyl chloride (3 mL, 6 eq) in 14 mL of THF was added dropwise. After that, the reaction system continues to react at low temperature for another 1 h. Finally, the solvents were evaporated to dryness under reduced pressure and the dried product was directly subjected to the next reaction without purification. (1.6 g, 72%)

Synthesis of peracetylated *N*-(prop-2-enoyl)- β -D-galactopyranosylamine 5. The dried galactosamine obtained above were dissolved in 200 mL of pyridine solution in a round-bottomed flask and 100 mL of acetic anhydride were subsequently added. The mixture was stirred at room temperature for 24 h, the reaction solution was evaporated under reduced pressure, after which TLC indicated 80%–90% conversion. The mixture dissolved in CH₂Cl₂ was filtered and washed with 150 mL CH₂Cl₂ thrice. The mixture was concentrated and purified by column chromatography, yield white crystals (2.37 g, 88.2%). ¹H NMR (500 MHz, CDCl₃): δ 6.41 (d, *J* = 9.2 Hz, 1H), 6.30 (d, *J* = 17.1 Hz, 1H), 6.06 (dd, *J* = 17.1, 10.4 Hz, 1H), 5.74 (d, *J* = 10.5 Hz, 1H), 5.45 (d, *J* = 1.2 Hz, 1H), 5.36 – 5.27 (m, 1H), 5.19 – 5.05 (m, 2H), 4.18 – 4.02 (m, 3H), 2.15 (s, 3H), 2.04 (d, *J* = 3.7 Hz, 6H), 2.00 (s, 3H).

Deprotection of the peracetylated (*N*-(prop-2-enoyl)- β -D-galactopyranosylamine).

Typically, the peracetylated *N*-(prop-2-enoyl)- β -D-galactopyranosylamine (0.05 g) were dissolved in THF, then 25% tetrabutylammonium hydroxide (TBAOH) was added in the solution dropwise and adjusted the pH of the solution to 9–10, TLC indicated full conversion within 10 min. The resultant mixture was evaporated under reduced pressure to remove the THF and then extracted with CH_2Cl_2 until the by-product had completely transferred from the aqueous layer to the organic layer. Finally, the water layer was evaporated under reduced pressure, yielding a white solid (0.028 g, 96 %). ^1H NMR (500 MHz, D_2O): δ 6.35 (dd, $J = 11.4, 6.9$ Hz, 1H), 5.90 (dd, $J = 6.7, 4.7$ Hz, 1H), 5.04 (t, $J = 9.2$ Hz, 1H), 4.02 (t, $J = 8.6$ Hz, 1H), 3.83 (t, $J = 5.9$ Hz, 1H), 3.76 (t, $J = 8.9$ Hz, 2H).

2.2 ^1H NMR spectrum of related Compounds

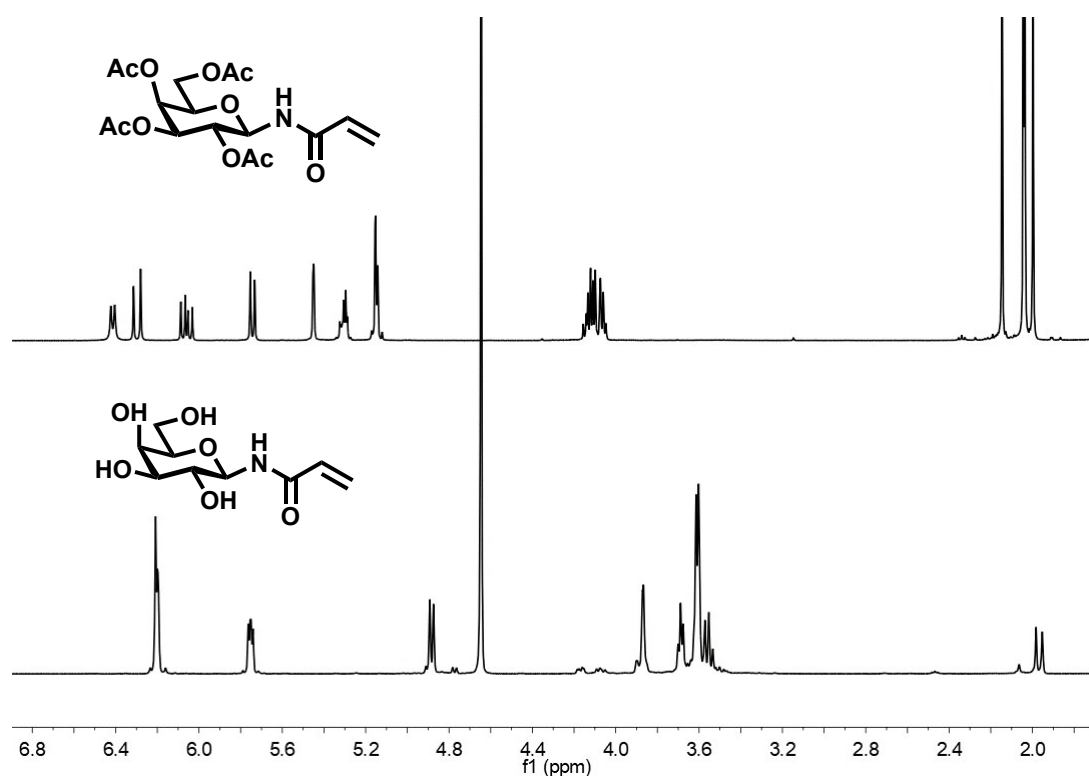


Fig. S1 ^1H NMR spectrum of peracetylated (*N*-(prop-2-enoyl)- β -D-galactopyranosylamine) and *N*-(prop-2-enoyl)- β -D-galactopyranosylamine.

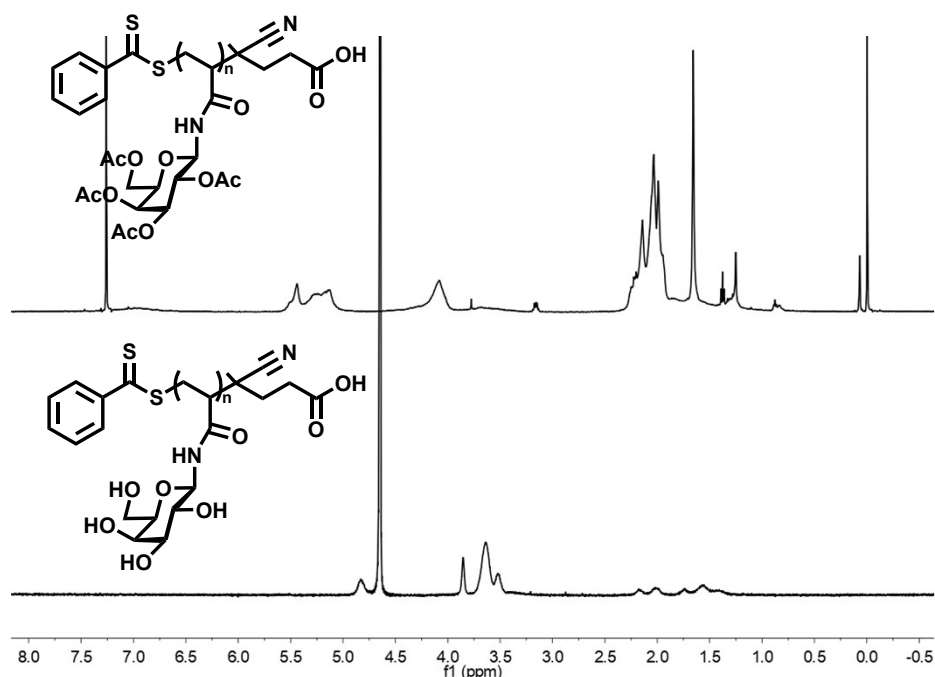


Fig. S2 ^1H NMR spectrum of $p\text{Gal}(\text{Ac})_m$ and $p\text{Gal}(\text{OH})_m$.

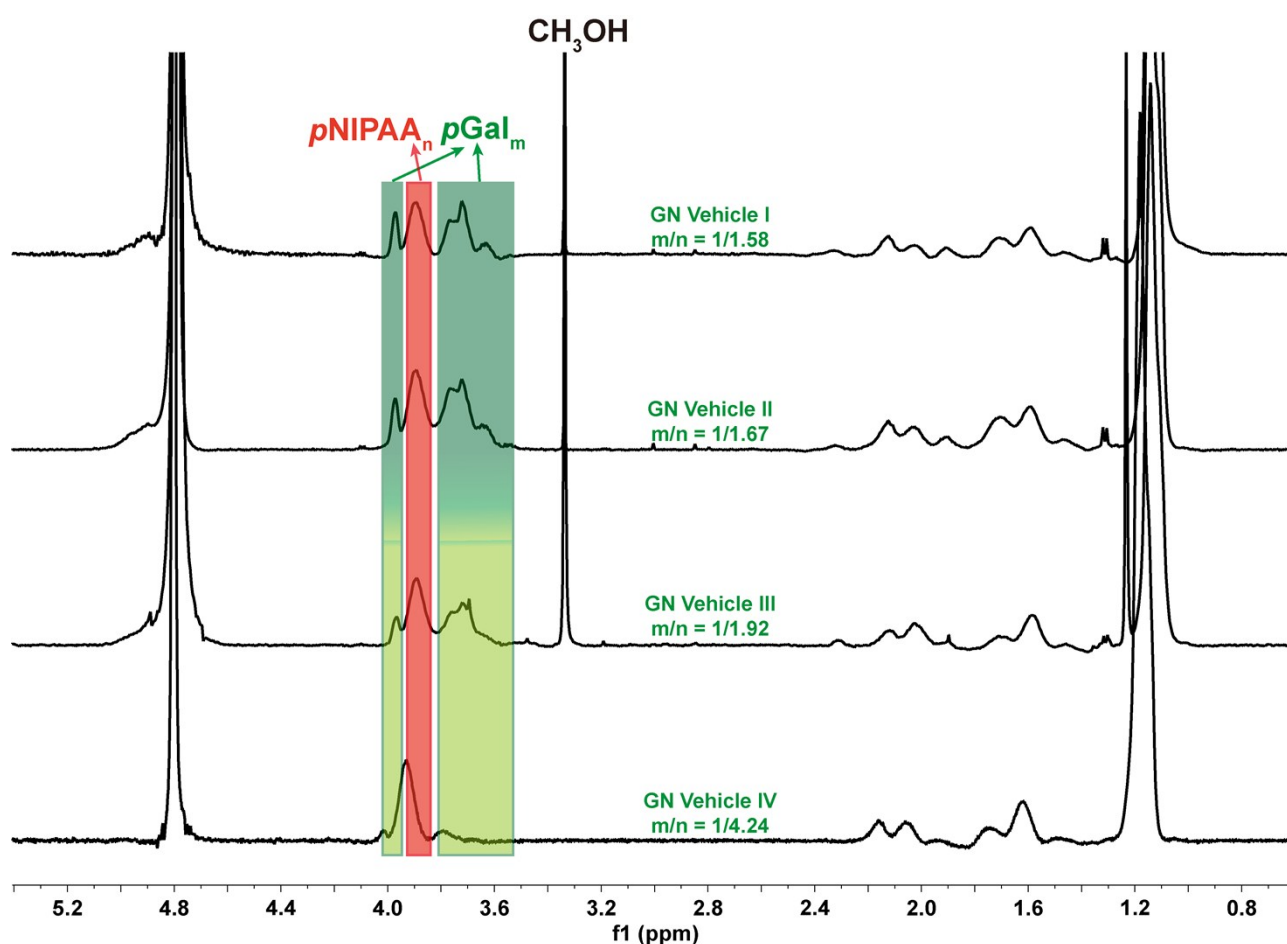


Fig. S3 ^1H NMR spectrum of a series of $p\text{Gal}(\text{OH})_m$ - b - $p\text{NIPAA}_n$. The ratio of galactose and NIPAA was determined by ^1H NMR integration of $p\text{Gal}(\text{OH})_m$ signal (δ 3.50~4.00 ppm minus amino-linked tertiary carbon signal, 3.89 ppm) to methyl signal (1.20 ppm).

3. Temperature sensitivity of GN Vehicle III.

10 mg/mL GN Vehicle III micellar solution was prepared as a stock solution that was diluted to a concentration of 0.625, 1.25, 2.5, 10 mg/mL using PBS buffer with pH 7.4, then, 200 μ L of different concentration of standard solution was accurately transferred to a transparent 96-well plate and the absorbance was measured at the wavelength of 492 nm by a microplate reader from 24 to 41 $^{\circ}$ C.

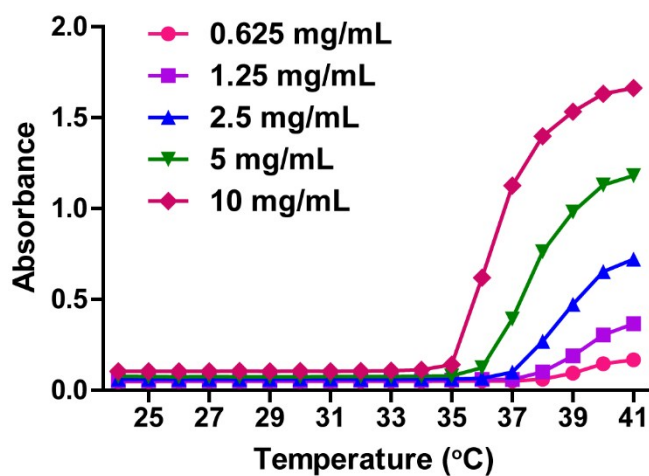


Fig. S4 Changes in absorbance of GN Vehicle III with different concentrations and temperature.

4. Quantitative analysis of doxorubicin

4.1 The method of quantitative analysis of doxorubicin

Absorbance and fluorescence intensity measurements were performed by microplate reader Tecan *SparkControl*[™] V2.3.5.

Quantitative analysis of high concentration doxorubicin by spectrophotometry

For acquiring absorbance linear regression equation, full-absorbance scanning about DOX solution was examined in the wavelength range of 280-800 nm using a microplate reader, while H₂O, DMSO and 1 mg/mL polymer micellar solution were used as controls. 2 mg/mL DOX was prepared as a stock solution that was diluted to a concentration of 50, 100, 150, 200, 250 and 300 µg/mL as DOX standard solution, then, 200 µL of different concentration of standard solution was accurately transferred to a transparent 96-well plate and the absorbance was measured at the optimal absorption wavelength of DOX by microplate reader. The linear regression equation between the absorbance and the concentration was obtained by taking concentration as the horizontal axis and absorbance as vertical axis using Excel.

For precision testing, accurately pipetting 200 µL of 50, 150, 300 µg/mL DOX standard solution to transparent 96-well plate as the representative of low, medium and high concentration to measure the absorbance (5 days, 5 times a day).

For recovery rate detection, 50, 150 and 300 µg/mL of doxorubicin solution was prepared using 1 mg/mL of the polymer vehicle as the solvent. The absorbance was measured at the optimal absorption wavelength of DOX (3 parallels per concentration), and the recovery rate was calculated in comparison with the absorbance standard concentration curve.

Quantitative analysis of low concentration doxorubicin by fluorescence spectrophotometry

For acquiring fluorescence linear regression equation, first, the fluorescent full scan about DOX solution was examined with excitation wavelength of 450~520 nm and emission wavelength of 540~620 nm to get the optimal condition to determine the concentration of DOX. Then, the fluorescence intensity of DOX was measured with a fixed excitation wavelength of 488 nm and the emission wavelength range of 300 to 550 nm, while H₂O, DMSO and 1 mg/mL polymer micellar solution were used as controls. 100 µg/mL DOX was prepared as a stock solution that was diluted to a concentration of 0.01, 0.05, 0.1, 0.2, 0.4, 0.6, 0.8 µg/mL as DOX standard solution respectively using PBS buffer at pH 7.4 and 5.5. Then, 200 µL of different concentration of standard solution was accurately transferred to a black 96-well plate and the fluorescence was measured at the optimal wavelength of DOX by a microplate reader. The linear regression equation between the fluorescence and the concentration indifferent pH condition was obtained by taking concentration as the horizontal axis and absorbance as vertical axis using Excel.

For precision testing, accurately pipetting 200 µL of 0.05, 0.2 and 0.6 µg/mL DOX standard solution to black 96-well plate as the representative of low, medium and high concentration to measure the fluorescence intensity (5 days, 5 times a day), and the precision was calculated in comparison with the fluorescence standard concentration curve.

4.2 Data about quantitative analysis of doxorubicin

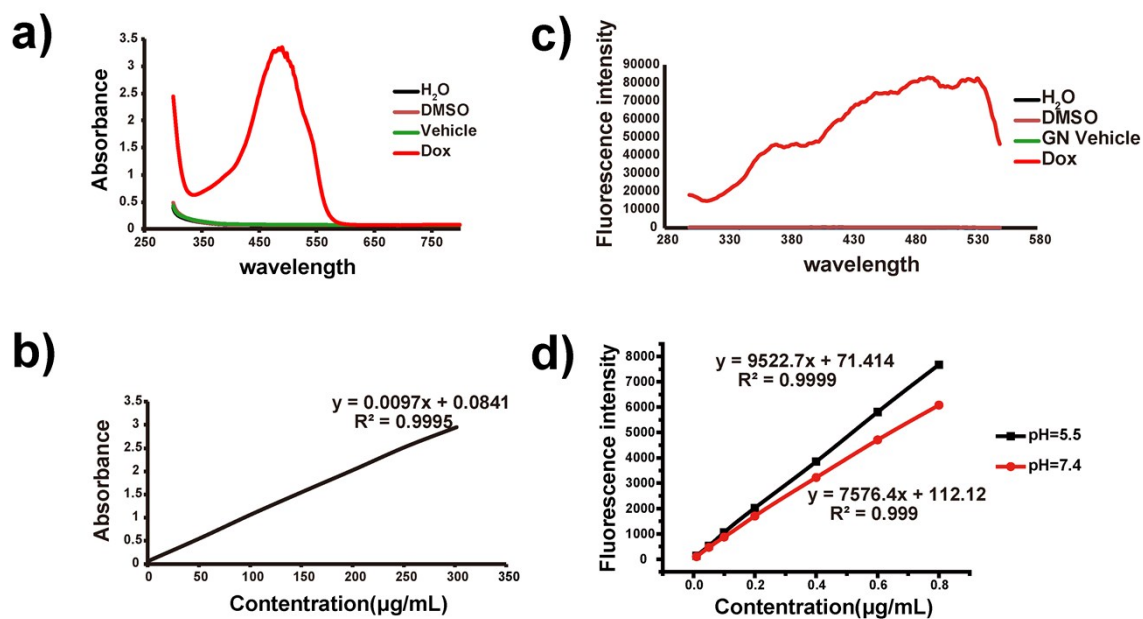


Fig. S5 Result about quantitative analysis of doxorubicin. (A) Absorbance full scan of doxorubicin, H₂O, DMSO, and GN Vehicle III (280-800 nm). (B) The standard curve for the quantification of doxorubicin (484 nm, $y = 0.0097x + 0.0841$, $R^2 = 0.995$). (C) Fluorescence scanning of doxorubicin, H₂O, DMSO, and GN Vehicle III with a fixed excitation wavelength of 488 nm and a wavelength range of 300 to 550 nm. (D) The standard curve for the quantification of doxorubicin in the buffer of pH 7.4 (red, $y = 7576.4x + 112.12$, $R^2 = 0.999$) and pH 5.5 (black, $y = 9522.7x + 71.414$, $R^2 = 0.9999$) at the excitation wavelength 484 nm and the emission wavelength 594 nm.

Tab. S1 Results of recovery rate about the concentration of doxorubicin determined with absorbance spectrophotometry.

Theoretical concentration ($\mu\text{g/mL}$)	Measured concentration ($\mu\text{g/mL}$)	Recovery rate (%)	Mean \pm SD	RSD (%)
50	50.16	100.33%	50.43 \pm 0.20	0.40
	50.47	100.95%		
	50.66	101.32%		
150	146.61	97.74%	146.53 \pm 0.07	0.05
	146.44	97.63%		
	146.54	97.69%		
300	290.01	96.67%	286.46 \pm 3.89	1.36
	288.33	96.11%		0.40
	281.05	93.68%		

Tab. S2 Results about determination of concentration of doxorubicin standard curve determined with absorbance spectrophotometry.

Concentration ($\mu\text{g/mL}$)	Intraday precision (n=5)			Interday precision (n=5)		
	A	Mean \pm SD	RSD(%)	A	Mean \pm SD	RSD(%)
50	0.562			0.554		
	0.557			0.570		
	0.564	0.561 \pm 0.003	0.576	0.567	0.567 \pm 0.007	1.368
	0.558			0.569		
	0.565			0.575		
150	1.543			1.556		
	1.536			1.575		
	1.556	1.538 \pm 0.011	0.772	1.531	1.555 \pm 0.017	1.191
	1.531			1.543		
	1.524			1.571		
300	2.949			2.949		
	2.955			2.985		
	2.950	2.962 \pm 0.018	0.593	3.035	2.992 \pm 0.033	1.114
	2.996			3.016		
	2.959			2.978		

Tab. S3 Results of intraday and interday precision about concentration of doxorubicin determined with fluorescence spectrophotometry.

Conditio n	Concentratio n	Intraday precision (n=5)			Daytime precision (n=5)							
		F	Mean±SD	RSD(%)	F	Mean±SD	RSD					
pH 5.5	0.05	523	526.4±19.22	3.65	523	535.4±17.17	3.20					
		515			557							
		561			514							
		504			554							
		529			529							
		2022			2022							
	0.2	1976	2033.2±39.29	1.93	2105	2063.0±36.91	1.79					
		2060			2048							
		2091			2031							
		2017			2109							
		5805			5805							
		0.6			5818			5734.20±65.0 6	1.13	5815	5871.8±100.74	1.72
					5699					6071		
					5694					5850		
5655	5818											
<hr/>												
pH 7.4	0.05		466	465.2±4.26	0.92	466	465.4±8.94			1.92		
		459	472									
		471	463									
		468	450									
		462	476									
		1702	1702									
	0.2	1721	1691.6±32.90	1.95	1703	1700.2±45.16	2.66					
		1696			1781							
		1628			1655							
		1711			1660							
		4707			4707							
		0.6			4628			4652.6±81.3	1.75	4747	4585.0±135.85	2.96
					4731					4597		
					4692					4377		
4505	4497											

5. In vitro biocompatibility evaluation

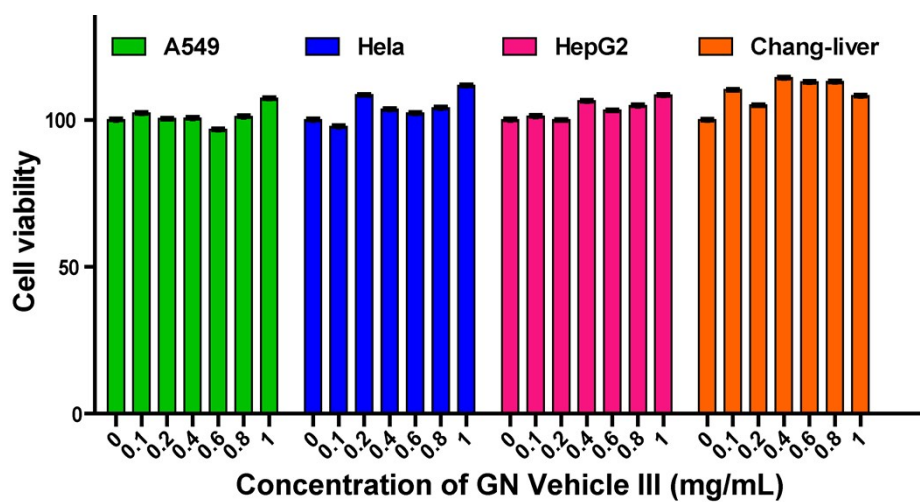


Fig. S6 Cell viability assay for GN Vehicle III with A549, HeLa, HepG2 and Chang-liver cells after 72 h incubation ($n \geq 3$).

6. In vivo activity evaluation

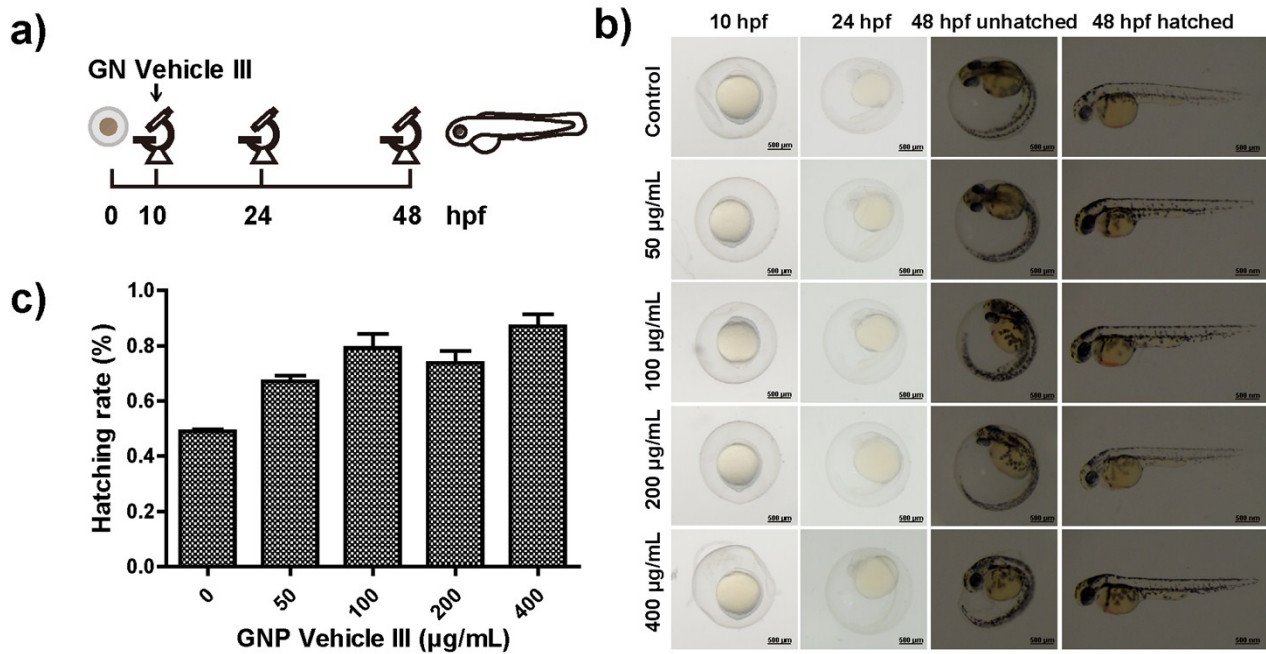


Fig. S7 (a) Schematic illustration of experiment procedure to study the hatching rates of zebrafish embryos following exposure to GN vehicle III. (b) Phenotype of zebrafish embryos following exposure to GN vehicle III. (c) The hatching rates of zebrafish embryos following exposure to GN vehicle III at 48 hpf, values are means \pm SD. The results are from at least three independent experiments, (n=102).

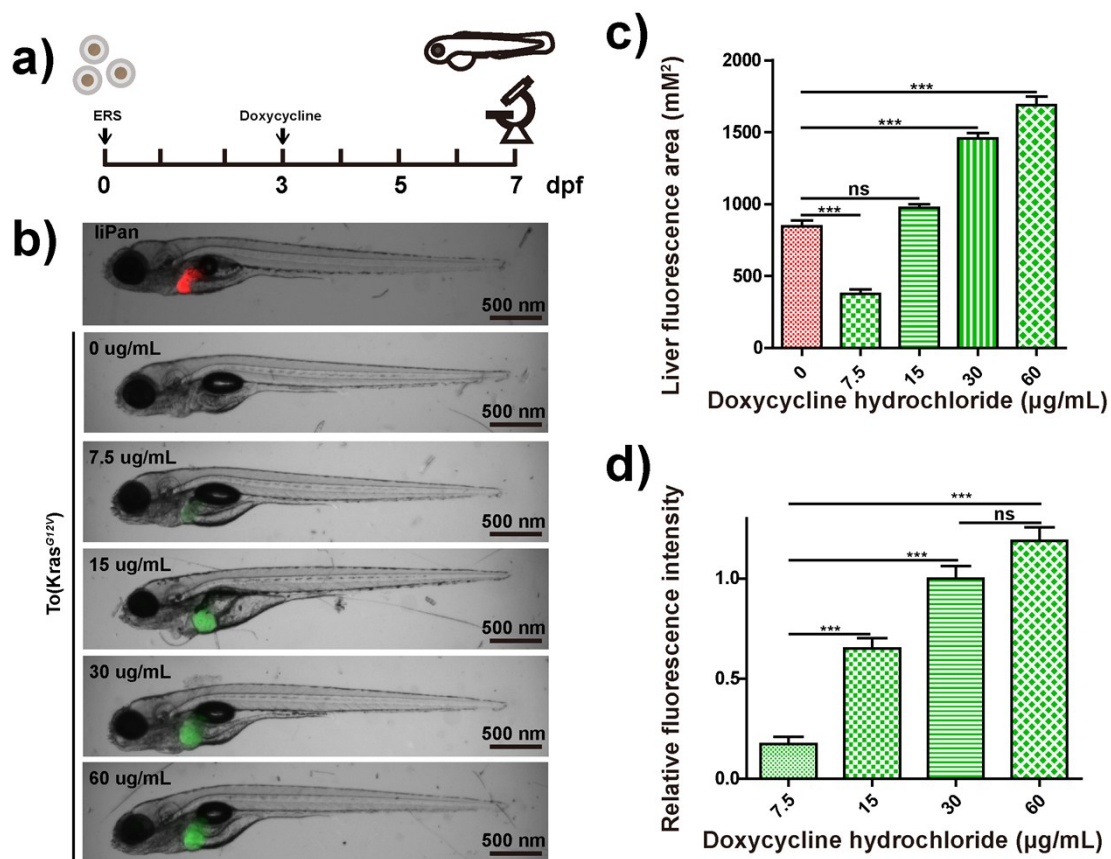


Fig. S8 Construction of the zebrafish liver cancer model. (a) Schematic illustration of experiment procedure to construct HCC model on To(Kras^{G12V}) zebrafish. (b) Phenotype of zebrafish embryos following exposure to doxycycline hydrochloride. (c) Liver fluorescence area and (d) Relative fluorescence intensity of the liver for the different concentration of doxycycline hydrochloride exposure from 3 dpf to 7 dpf. The results are from at least three independent experiments and values are means \pm SD. * $p < 0.05$; ** $p < 0.01$; *** $p < 0.001$. Unpaired t-test, two-tailed (n=30).

7. Reference

- 1 T. W. Chew, X. J. Liu, L. Liu, J. M. Spitsbergen, Z. Gong and B. C. Low, *Oncogene*, 2014, **33**, 2717-2727.
- 2 L. M. Likhoshesterov, O. S. Novikova and V. N. Shibaev, *Dokl. Chem.*, 2002, **383**, 89.
- 3 J. Tang, E. Ozhegov, Y. Liu, D. Wang, X. Yao and X.-L. Sun, *ACS Macro Lett.*, 2017, **6**, 107-111.